

Improving cutoff frequency estimation via optimized π-pulse sequence

Wang-Sheng Zheng(郑王升), Chen-Xia Zhang(张晨霞), and Bei-Li Gong(龚贝利)

Citation: Chin. Phys. B, 2025, 34 (**1**): 010309. DOI: 10.1088/1674-1056/ad9ba1
Journal homepage: http://cpb.iphy.ac.cn; http://iopscience.iop.org/cpb

What follows is a list of articles you may be interested in

Quantum-enhanced interferometry with unbalanced entangled coherent states

Jun Tang(汤俊), Zi-Hang Du(堵子航), Wei Zhong(钟伟), Lan Zhou(周澜), and Yu-Bo Sheng(盛宇波)
Chin. Phys. B, 2025, 34 (**1**): 020303. DOI: 10.1088/1674-1056/ad99ca

Parameter estimation in n-dimensional massless scalar field

Ying Yang(杨颖) and Jiliang Jing(荆继良)
Chin. Phys. B, 2024, 33 (**3**): 030307. DOI: 10.1088/1674-1056/ad1749

Holevo bound independent of weight matrices for estimating two parameters of a qubit

Chang Niu(牛畅) and Sixia Yu(郁司夏)
Chin. Phys. B, 2024, 33 (**2**): 020304. DOI: 10.1088/1674-1056/ad117d

Quantum interferometric power and non-Markovianity in the decoherence channels

Shaojie Xiong(熊少杰), Zhe Sun(孙哲), and Xiaoguang Wang(王晓光)
Chin. Phys. B, 2023, 32 (**8**): 080302. DOI: 10.1088/1674-1056/accb4e

Improving the teleportation of quantum Fisher information under non-Markovian environment

Yan-Ling Li(李艳玲), Yi-Bo Zeng(曾艺博), Lin Yao(姚林), and Xing Xiao(肖兴)
Chin. Phys. B, 2023, 32 (**1**): 010303. DOI: 10.1088/1674-1056/ac6497

Improving cutoff frequency estimation via optimized π-pulse sequence

Wang-Sheng Zheng(郑王升)[1], Chen-Xia Zhang(张晨霞)[2], and Bei-Li Gong(龚贝利)[1,†]

[1] *School of Electrical Engineering, Guangxi University, Nanning* 530004, *China*

[2] *Faculty of Science and Technology, College of Arts and Sciences of Hubei Normal University, Huangshi* 435109, *China*

(Received 19 August 2024; revised manuscript received 30 October 2024; accepted manuscript online 9 December 2024)

The cutoff frequency is one of the crucial parameters that characterize the environment. In this paper, we estimate the cutoff frequency of the Ohmic spectral density by applying the π-pulse sequences (both equidistant and optimized) to a quantum probe coupled to a bosonic environment. To demonstrate the precision of cutoff frequency estimation, we theoretically derive the quantum Fisher information (QFI) and quantum signal-to-noise ratio (QSNR) across sub-Ohmic, Ohmic, and super-Ohmic environments, and investigate their behaviors through numerical examples. The results indicate that, compared to the equidistant π-pulse sequence, the optimized π-pulse sequence significantly shortens the time to reach maximum QFI while enhancing the precision of cutoff frequency estimation, particularly in deep sub-Ohmic and deep super-Ohmic environments.

Keywords: environment parameters estimation, quantum Fisher information, optimized π-pulse sequence

PACS: 03.65.Yz, 03.67.–a, 06.20.–f

DOI: 10.1088/1674-1056/ad9ba1 **CSTR:** 32038.14.CPB.ad9ba1

1. Introduction

Realistic quantum systems are regarded as open systems due to the non-negligible environment-induced effects.[1] The interactions between the systems and their surrounding environments lead to quantum decoherence, which plays an important role in quantum information theory.[2] To understand quantum dynamics properly, the environment parameters that govern the decoherence function are required to be estimated with high precision. The study on the estimation of environment parameters has drawn great attention recently.[3–6] One critical parameter is the cutoff frequency, which determines the correlation timescale of the environment.[7] Therefore, how to precisely estimate the cutoff frequency becomes one of the indispensable ingredients for implementing practical quantum technologies.

Typically, the cutoff frequency of the environment can be effectively estimated by means of the quantum probe, which is a small and easily controllable system.[8] In general, a complete quantum parameter estimation scheme can be divided into the following four steps:[9] (i) preparation of the probe state; (ii) evolution; (iii) measurement, and (iv) classical estimation. There have been several approaches to achieve better precision in parameter estimation for different steps. For step (i), the continuous-variable probe,[10] the dissipating probe,[11] the two-qubit probe,[12] and the initial probe-environment correlation[13] have been considered in estimating the cutoff frequency. For step (ii), additional control methods are usually applied to alter the dynamics of the probe for improvement of the precision limit, e.g., feedback control,[14–16] optimal control,[17,18] Hamiltonian control,[19] and dynamical control.[20] Dynamical control is originally presented as a strategy for fighting decoherence in open quantum systems through open-loop control technologies.[21] Two common ways for dynamical control are with the application of the equidistant and the optimized π-pulse sequence. The equidistant π-pulse sequence has been proved to be effective in increasing the precision of estimating cutoff frequency in Ref. [13], where the authors took into account the control field to enable the probe to collect more information about the environment before the probe completely decoheres. By relaxing the constraint of uniform pulse intervals, the optimized π-pulse sequence achieves higher-order decoupling of the environment with fewer pulses compared to the equidistant sequence.[22] The superiority of the optimized π-pulse sequence has been demonstrated for the transitions suppression,[23] the transverse relaxation time measurement,[24] the phase parameter estimation,[25] and the generation of entangling gates.[26] Since the optimized π-pulse sequence has shown notable impacts on various quantum tasks, it can be expected to enhance the precision of environment parameters estimation.

Inspired by Refs. [13,27], we apply the optimized π-pulse sequence to the quantum probe for the estimation of the cutoff frequency. We consider that the quantum probe couples to a bosonic environment characterized by the Ohmic spectral density and undergoes pure dephasing. The precision of esti-

†Corresponding author. E-mail: aublgong@gxu.edu.cn

© 2025 Chinese Physical Society and IOP Publishing Ltd. All rights, including for text and data mining, AI training, and similar technologies, are reserved.

mation is quantified by the quantum Fisher information (QFI) and quantum signal-to-noise ratio (QSNR). We provide the analytical forms of QFI and QSNR of estimating the cutoff frequency with the application of the optimized π-pulse sequence, then analyze their behaviors compared with the cases where applying no pulses and the equidistant π pulses through numerical examples. Specifically, we show and contrast the time evolution of QFI, the optimal interaction time (which can be found by maximizing the QFI over time), the maximum of QFI, and the QSNR for different environments. It is demonstrated that compared to the cases of applying the equidistant π-pulse sequence, an increase in the maximum of QFI and a decrease in the optimal interaction time can be obtained by applying the optimized π pulses. The effect of the optimized π-pulse sequence on the estimation precision of cutoff frequency is even more impressive in deep sub-Ohmic ($s < 0.5$)[28] and deep super-Ohmic ($s > 5$)[29] environments.

This paper is organized as follows. Section 2 briefly introduces the physical model of the quantum probe coupled with a bosonic environment. Under this model, the QFI and QSNR are derived in Section 3 for the evaluation of estimating the cutoff frequency. We present numerical results of the QFI and QSNR in Section 4. Finally, the conclusion is summarized in Section 5.

2. The physical model

We aim to investigate how the optimized π-pulse sequence applied to the quantum probe affects the estimation of the cutoff frequency. The probe we consider is a two-level system undergoing pure dephasing via interaction with a bosonic environment. As illustrated in Fig. 1, we apply the optimized π-pulse sequence to modulate the interaction between the probe and the environment.

Let $\gamma(z,n)$ denote the π-pulse sequence, the global modulated Hamiltonian can be written as (we set $\hbar = 1$ throughout)[13]

$$H = \frac{\omega_0}{2}\gamma(z,n)\sigma_z + \sum_k \omega_k b_k^\dagger b_k + \sum_k \gamma(z,n)\sigma_z(g_k b_k^\dagger + g_k^* b_k).$$

Here, σ_z is the Pauli matrix, ω_0 is the energy spacing of the probe, and k labels the modes of the environment with frequency ω_k, the interaction strength g_k, and bosonic creation (annihilation) operator $b_k^\dagger$ (b_k), satisfying the commutation relation $[b_k, b_{k'}^\dagger] = \delta_{kk'}$. With n the number of pulses, the function of the optimized π-pulse sequence is given by[13,30]

$$\gamma(z,n) = \sum_{j=0}^{n}(-1)^j \Theta(z - t_j)\Theta(t_{j+1} - z), \tag{1}$$

where the total time interval $0 \to t$ is split into smaller intervals $0 \to t_1 \to t_2 \to \cdots \to t_n \to t$, $t_j = t\sin^2[\pi j/(2n+2)]$, $z \in [0,t]$, and $\Theta(x)$ is the sign function:

$$\Theta(x) = \begin{cases} +1, & x > 0, \\ -1, & x < 0. \end{cases}$$

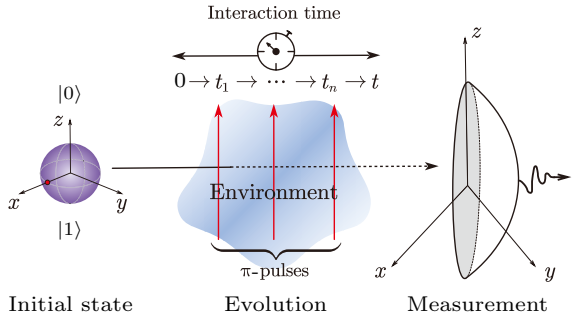


Fig. 1. Schematic diagram of estimating the cutoff frequency. The optimized π-pulse sequence is applied in a given optimal interaction time, and a set of measurements is performed on the final probe state to extract the information about the environment.

Complete information about the interaction between the environment and the probe can be encapsulated in the spectral density. In this work, we consider that the spectral density belongs to the Ohmic class with an exponential frequency cutoff, which can simulate a large class of thermal bath and model many real systems:[31–35]

$$J(\omega) = G\frac{\omega^s}{\omega_c^{s-1}}\exp\left(-\frac{\omega}{\omega_c}\right). \tag{2}$$

In Eq. (2), G is the coupling strength of the environment, which carries the order of magnitude of g_k,[36,37] ω_c is the cutoff frequency, and s is the Ohmicity parameter, which distinguishes between sub-Ohmic ($s < 1$), Ohmic ($s = 1$), and super-Ohmic ($s > 1$) regimes. According to the spectral density, we can calculate the reduced dynamics of the probe in the interaction picture.[38] Suppose the initial state of the probe is independent of the environment, which means the total initial state is a product state $\rho_{\rm tot} = \rho(0) \otimes \rho_{\rm E}$, with the initial probe state $\rho(0)$ and the environment thermal equilibrium state $\rho_{\rm E} = {\rm e}^{-H_{\rm E}/T}/{\rm Tr}_{\rm E}[{\rm e}^{-H_{\rm E}/T}]$.[39] Here T is the temperature, $H_{\rm E}$ is the Hamiltonian of the environment, and ${\rm Tr}_{\rm E}$ is the environment partition function. With the application of an optimized π-pulse sequence, the probe state at time t can be expressed by[8]

$$\rho(t) = \begin{pmatrix} 1 & {\rm e}^{-{\rm i}\omega_0 t}{\rm e}^{-\Gamma_{\rm op}(t)} \\ {\rm e}^{{\rm i}\omega_0 t}{\rm e}^{-\Gamma_{\rm op}(t)} & 1 \end{pmatrix} \circ \rho(0), \tag{3}$$

where $\circ$ denotes the element-wise Hadamard product, and[27]

$$\Gamma_{\rm op}(t) = \int_0^\infty \frac{J(\omega)}{2\omega^2}\coth\left(\frac{\omega}{2T}\right)|y_n(\omega t)|_{\rm op}^2 {\rm d}\omega$$

is the decoherence function, whose factor $|y_n(\omega t)|_{\rm op}^2$ has the form

$$|y_n(\omega t)|_{\rm op}^2 = \left|\sum_{j=-n-1}^{n}(-1)^j {\rm e}^{({\rm i}\omega t/2)\cos[\pi j/(n+1)]}\right|^2.$$

If we use the equidistant π pulses, i.e., $t_j = tj/(n+1)$ in Eq. (1), the probe state is again obtained as Eq. (3), except for a modified decoherence function[13,27]

$$\Gamma_{\rm eq}(t) = \int_0^\infty \frac{J(\omega)}{2\omega^2} \coth\left(\frac{\omega}{2T}\right) |y_n(\omega t)|^2_{\rm eq} \, {\rm d}\omega$$

with

$$|y_n(\omega t)|^2_{\rm eq} = 2\tan^2\left(\frac{\omega t}{2n+2}\right)[1+(-1)^n\cos(\omega t)].$$

When we apply no pulses, the decoherence function is

$$\Gamma_{\rm uc}(t) = \int_0^\infty \frac{J(\omega)}{\omega^2}[1-\cos(\omega t)]\,{\rm d}\omega.$$

Below we provide tools that quantify the precision with which cutoff frequency can be estimated by the probe.

3. Quantum estimation theory

It is seen that the evolution of the probe state carries information about the environment, which implies the parameters that characterize the environment can be estimated from the dynamics of the probe. To infer the value of the cutoff frequency, we perform measurements on repeated preparations of the probe. The measurement outcomes are used to build an estimator $\hat{\omega}_{\rm c}$ of the cutoff frequency. The inevitable errors caused during the process of building the estimator can be quantified by the variance $\delta^2(\hat{\omega}_{\rm c})$, where the smaller is $\delta^2(\hat{\omega}_{\rm c})$, the more precise is the estimation strategy. For any unbiased estimator $\hat{\omega}_{\rm c}$, the precision is bounded by Cramér–Rao inequality:[40]

$$\delta^2(\hat{\omega}_{\rm c}) \geq \frac{1}{N\mathcal{F}(\omega_{\rm c})}. \tag{4}$$

Here N is the number of repeated measurements, and $\mathcal{F}(\omega_{\rm c})$ is the QFI. Equation (4) tells us that the optimal estimation strategy is to maximize the QFI and saturate the inequality. The QFI is generally defined as[41]

$$\mathcal{F}(\omega_{\rm c}) := {\rm Tr}\left[\rho(t)L^2_{\omega_{\rm c}}\right],$$

where $L_{\omega_{\rm c}}$ is the symmetric logarithmic derivative, satisfying

$$\frac{\partial\rho(t)}{\partial\omega_{\rm c}} = \frac{1}{2}\left[\rho(t)L_{\omega_{\rm c}} + L_{\omega_{\rm c}}\rho(t)\right].$$

If the probe state has spectral decomposition

$$\rho(t) = \sum_i p_i |\psi_i\rangle\langle\psi_i|,$$

where p_i is the i-th non-zero eigenvalue of the probe state and the corresponding eigenvector is $|\psi_i\rangle$, the explicit expression of the QFI can be found to be[42]

$$\begin{aligned}\mathcal{F}(\omega_{\rm c}) =& \sum_i \frac{(\partial p_i/\partial\omega_{\rm c})^2}{p_i} \\ &+ 2\sum_{i\neq j}\frac{(p_i-p_j)^2}{p_i+p_j}\left|\langle\psi_j|\frac{\partial|\psi_i\rangle}{\partial\omega_{\rm c}}\right|^2.\end{aligned} \tag{5}$$

We prepare the probe in the initial state

$$\rho(0) = \begin{pmatrix}\cos^2(\theta/2) & \frac{1}{2}\sin\theta{\rm e}^{-{\rm i}\phi} \\ \frac{1}{2}\sin\theta{\rm e}^{{\rm i}\phi} & \sin^2(\theta/2)\end{pmatrix},$$

which is parameterized by the polar angle $\theta\in[0,\pi/2]$ and the azimuthal angle $\phi\in[0,2\pi]$ on the Bloch sphere. From Eq. (3), after we apply the optimized π-pulse sequence to the probe, the probe state at a later time t reads

$$\rho(t) = \begin{pmatrix}\cos^2(\theta/2) & \frac{1}{2}\sin\theta{\rm e}^{-{\rm i}(\phi+\omega_0 t)}{\rm e}^{-\Gamma_{\rm op}(t)} \\ \frac{1}{2}\sin\theta{\rm e}^{{\rm i}(\phi+\omega_0 t)}{\rm e}^{-\Gamma_{\rm op}(t)} & \sin^2(\theta/2)\end{pmatrix}. \tag{6}$$

From Eq. (6), the eigenvalues and eigenvectors of the probe state are obtained as

$$p_1 = \frac{1}{2}[1-\mathcal{Q}(t)], \tag{7a}$$

$$p_2 = \frac{1}{2}[1+\mathcal{Q}(t)], \tag{7b}$$

$$|\psi_1\rangle = \cos(\bar{\theta}/2)|0\rangle - \sin(\bar{\theta}/2){\rm e}^{-{\rm i}(\phi+\omega_0 t)}|1\rangle, \tag{8a}$$

$$|\psi_2\rangle = \sin(\bar{\theta}/2)|0\rangle + \cos(\bar{\theta}/2){\rm e}^{-{\rm i}(\phi+\omega_0 t)}|1\rangle, \tag{8b}$$

where we denote

$$\mathcal{Q}(t) = \sqrt{1+\sin^2\theta({\rm e}^{-2\Gamma_{\rm op}(t)}-1)}, \tag{9}$$

$$\sin\bar{\theta} = \sin\theta[\mathcal{Q}(t)]^{-1}{\rm e}^{-\Gamma_{\rm op}(t)}, \tag{10a}$$

$$\cos\bar{\theta} = \cos\theta[\mathcal{Q}(t)]^{-1}. \tag{10b}$$

According to Eqs. (7)–(10), we are further led to

$$\begin{aligned}\left(\frac{\partial p_1}{\partial\omega_{\rm c}}\right)^2 &= \left(\frac{\partial p_2}{\partial\omega_{\rm c}}\right)^2 \\ &= \frac{1}{4}[\mathcal{Q}(t)]^{-2}\sin^4\theta{\rm e}^{-4\Gamma_{\rm op}(t)}\left[\frac{\partial\Gamma_{\rm op}(t)}{\partial\omega_{\rm c}}\right]^2,\end{aligned} \tag{11}$$

$$\left|\langle\psi_2|\frac{\partial|\psi_1\rangle}{\partial\omega_{\rm c}}\right|^2 = \left|\langle\psi_1|\frac{\partial|\psi_2\rangle}{\partial\omega_{\rm c}}\right|^2 = \frac{1}{4}\left(\frac{\partial\bar{\theta}}{\partial\omega_{\rm c}}\right)^2, \tag{12}$$

where the partial derivative of $\bar{\theta}$ with respect to $\omega_{\rm c}$ can be derived from Eq. (10)

$$\frac{\partial\bar{\theta}}{\partial\omega_{\rm c}} = -\sin\theta\cos\theta[\mathcal{Q}(t)]^{-2}{\rm e}^{-\Gamma_{\rm op}(t)}\frac{\partial\Gamma_{\rm op}(t)}{\partial\omega_{\rm c}}. \tag{13}$$

By substituting Eqs. (11)–(13) into Eq. (5), we find that the QFI of estimating cutoff frequency with the application of the optimized π-pulse sequence is

$$\mathcal{F}_{\rm op}(\omega_{\rm c}) = \frac{\sin^2\theta}{{\rm e}^{2\Gamma_{\rm op}(t)}-1}\left[\frac{\partial\Gamma_{\rm op}(t)}{\partial\omega_{\rm c}}\right]^2. \tag{14}$$

In addition to QFI, we quantify the precision of an estimator through the QSNR with the expression[11]

$$\mathcal{R}_{\rm op}(\omega_{\rm c}) = \mathcal{F}_{\rm op}(\omega_{\rm c})\omega_{\rm c}^2. \tag{15}$$

As a global estimability, a larger value of the QSNR means a more efficient estimate with smaller error.[43] By modifying the decoherence function, equations (14) and (15) can also be used to calculate the QFI and QSNR with no pulses and the equidistant π pulses applied correspondingly. The QFI and QSNR are the main tools that we use in the following discussion.

4. Numerical examples

We now investigate the precision in estimating the cutoff frequency with the optimized π-pulse sequence applied at zero temperature. To this end, we analyze the behaviors of the QFI and QSNR numerically, and compare them to the cases of applying no pulses and the equidistant π pulses for different environments. Note that the QFI is a decreasing function with respect to $\theta \in [0, \pi/2]$, and irrelevant to ϕ. Throughout we set $\theta = \phi = 0$, $\omega_0 = 1$, and the Ohmicity parameter $s = 0.1$, 1, and 3 for the sub-Ohmic, Ohmic, and super-Ohmic environments.

The QFI is a function of the decoherence function of the quantum probe, thus a function of the interaction time. To optimize the estimation process, the maximization of the QFI is performed over time to determine the maximum of QFI and the corresponding optimal interaction time $t^{\rm opt}$. Here we give examples of the decoherence function and QFI for different control pulses and different environments with $G = 1$, $\omega_{\rm c} = 1$, and $n = 3$. As plotted in Figs. 2 and 3, the dotted, dashed, and solid lines indicate the cases with no pulses, the equidistant π pulses, and the optimized π pulses applied, respectively. One can see that both π-pulse sequences suppress the decoherence function for a period of time, within which the QFI reaches its maximal value. In Fig. 3, the solid line always has the highest peak, which means that by modulating the interaction between the probe and the environment with the optimized π-pulse sequence for a proper time, we have a larger QFI when estimating cutoff frequency.

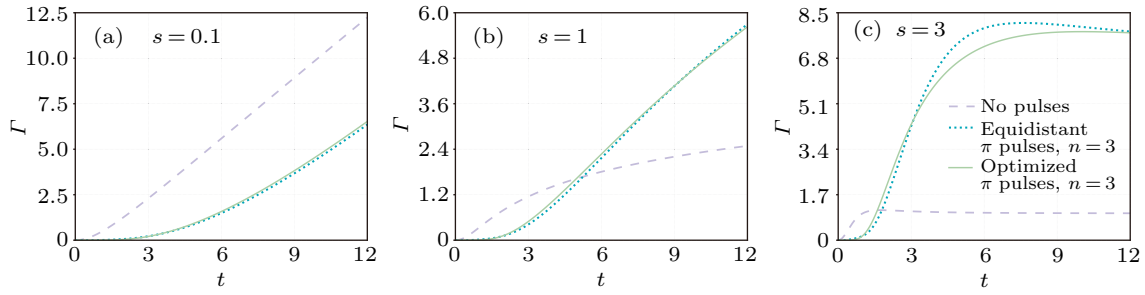


Fig. 2. The decoherence function in (a) sub-Ohmic, (b) Ohmic, (c) super-Ohmic environment with $G = 1$, $\omega_{\rm c} = 1$, and $n = 3$.

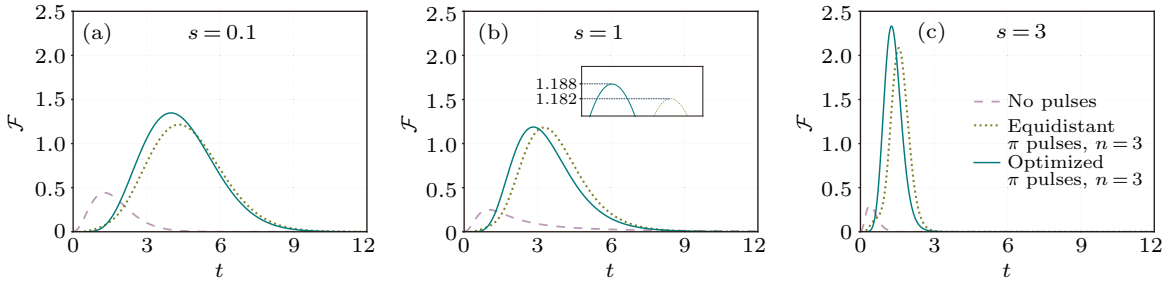


Fig. 3. Time evolution of the QFI in (a) sub-Ohmic, (b) Ohmic, (c) super-Ohmic environment with $G = 1$, $\omega_{\rm c} = 1$, and $n = 3$.

Under the condition of each probe interacting with the environment for the optimal time, we illustrate the maximum of QFI and the optimal interaction time with $G = 1$ in Fig. 4. It shows that both the maximum of QFI and the optimal interaction time increase with the number of pulses and decrease as $\omega_{\rm c}$ increases, which is expected since the pulses suppress the decoherence, while more modes contribute to the decoherence with increasing $\omega_{\rm c}$.[13] In the upper row of Fig. 4, the red crosses (representing the optimized π-pulse sequence) are always above the green dots (representing the equidistant π pulses) and the blue triangles (representing no pulses) with $n = 3$. As the number of pulses varies with $\omega_{\rm c} = 1$, both red crosses and the green dots are above the blue triangles (see the lower row of Fig. 4), where the red crosses are located higher in the sub-Ohmic environment; the green dots are located higher in the Ohmic environment except for $n = 3$; the

red crosses are located higher in the super-Ohmic environment except for $n = 2$. In our experiments, the maximal values of the QFI in the sub-Ohmic and super-Ohmic environments with the optimized π-pulse sequence applied are on average 9.95% and 11.48% higher than that with the equidistant π-pulse sequence applied, respectively. However, the solid line stays below the dashed line in every sub-figure. Specifically, the QFI with the optimized π-pulse sequence applied takes on average 14.35% less time to reach the maximum. In summary, the optimized π-pulse sequence, within a shorter interaction time, helps us in achieving a greater value of the maximal QFI for any ω_c when $n = 3$, and improves the estimation of cutoff frequency in the sub-Ohmic and super-Ohmic environment for $n \geq 3$ when $\omega_c = 1$.

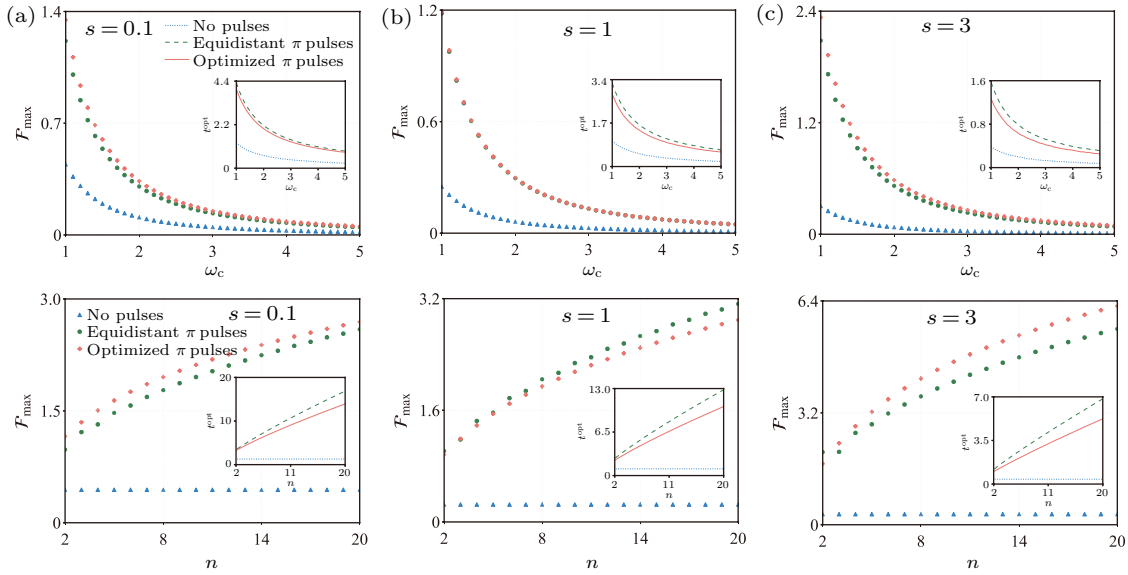


Fig. 4. The maximum of QFI and the corresponding optimal interaction time, as functions of the cutoff frequency (the upper row, with $n = 3$) and the number of pulses (the lower row, with $\omega_c = 1$) in (a) sub-Ohmic, (b) Ohmic, (c) super-Ohmic environment with $T = 0$ and $G = 1$.

Additionally, the dependencies of the QSNR on ω_c and s with $G = 1$, $n = 3$ are depicted in Fig. 5. Figure 5(b) is a sample of Fig. 5(a) by taking $s = 3$, where the main feature is that the value of QSNR is irrelevant to ω_c. Figure 5(c) suggests that the optimized π-pulse sequence offers a larger QSNR than the equidistant π-pulse sequence except for approximately $1.2 < s < 2.1$, where we can obtain significant advantages for deep sub-Ohmic and deep super-Ohmic regimes.

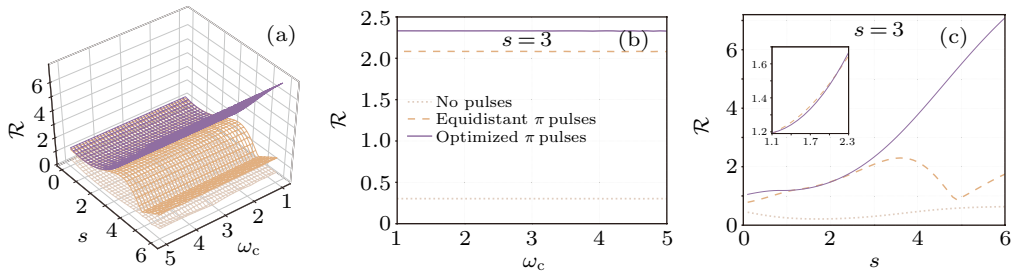


Fig. 5. Comparing the dependencies of the QSNR on (a) ω_c and s, (b) ω_c (with $s = 3$), (c) s, with $T = 0$, $G = 1$, and $n = 3$.

With these numerical results in hand, it is found that the QFI increases with the number of pulses, and is inversely proportional to ω_c^2. We conclude that the optimized π-pulse sequence plays a big role in the deep sub-Ohmic and deep super-Ohmic environments, allowing us to estimate the cutoff frequency more precisely.

5. Conclusions

In this paper, we have applied the optimized π-pulse sequence to the quantum probe to improve the estimation of the cutoff frequency of the environment. Considering a physical model where the quantum probe interacts with a bosonic environment, the analytical forms of the QFI and QSNR have been derived as tools to quantify the precision of estimating the cutoff frequency. Through the numerical examples, we have found that in comparison with the equidistant π-pulse sequence, the optimized π-pulse sequence on average reduces the optimal interaction time by 14.35% across all environments, and increases the maximum of QFI by 9.95% and 11.48% in the sub-Ohmic and super-Ohmic environments, respectively. Further, the estimation precision of cutoff frequency can be improved even more significantly in a deep sub-

Ohmic or deep super-Ohmic regime.

Acknowledgements

Project supported by the National Natural Science Foundation of China (Grant No. 62403150), the Innovation Project of Guangxi Graduate Education (Grant No. YCSW2024129), and the Guangxi Science and Technology Base and Talent Project (Grant No. Guike AD23026208).

References

[1] Breuer H P and Petruccione F 2007 *The Theory of Open Quantum Systems* (New York: Oxford University Press)
[2] Paavola J, Piilo J, Suominen K A and Maniscalco S 2009 *Phys. Rev. A* **79** 052120
[3] Razavian S and Paris M G A 2019 *Physica A* **525** 825
[4] Gebbia F, Benedetti C, Benatti F, Floreanini R, Bina M and Paris M G A 2020 *Phys. Rev. A* **101** 032112
[5] Tamascelli D, Benedetti C, Breuer H P and Paris M G A 2020 *New J. Phys.* **22** 083027
[6] Zhang C and Gong B 2024 *Phys. Scr.* **99** 025101
[7] Tan Q S, Wu W, Xu L, Liu J and Kuang L M 2022 *Phys. Rev. A* **106** 032602
[8] Benedetti C, Salari Sehdaran F, Zandi M H and Paris M G A 2018 *Phys. Rev. A* **97** 012126
[9] Yang Y and Jing J 2024 *Chin. Phys. B* **33** 030307
[10] Bina M, Grasselli F and Paris M G A 2018 *Phys. Rev. A* **97** 012125
[11] Sehdaran F S, Zandi M H and Bahrampour A 2019 *Phys. Lett. A* **383** 126006
[12] Mirza A R and Chaudhry A Z 2024 *Sci. Rep.* **14** 6803
[13] Ather H and Chaudhry A Z 2021 *Phys. Rev. A* **104** 012211
[14] Liu L and Yuan H 2020 *Phys. Rev. A* **102** 012208
[15] Ji Y, Ke Q and Hu J 2020 *Chin. Phys. B* **29** 120303
[16] Fallani A, Rossi M A C, Tamascelli D and Genoni M G 2022 *PRX Quantum* **3** 020310
[17] Liu J and Yuan H 2017 *Phys. Rev. A* **96** 012117
[18] Ansel Q, Dionis E and Sugny D 2024 *SciPost Phys.* **16** 013
[19] Gong B and Cui W 2018 *Sci. China Phys. Mech. Astron.* **61** 040312
[20] Zwick A, Álvarez G A and Kurizki G 2016 *Phys. Rev. Appl.* **5** 014007
[21] Viola L, Knill E and Lloyd S 1999 *Phys. Rev. Lett.* **82** 2417
[22] Zhen X L, Zhang F H, Feng G, Li H and Long G L 2016 *Phys. Rev. A* **93** 022304
[23] Schroeder C A and Agarwal G S 2011 *Phys. Rev. A* **83** 012324
[24] Chakraborty I, Chakrabarti A and Bhattacharyya R 2015 *Phys. Chem. Chem. Phys.* **17** 32384
[25] Ji Y and Hu J 2020 *Int. J. Theor. Phys.* **59** 1585
[26] Dong W, Calderon-Vargas F A and Economou S E 2020 *New J. Phys.* **22** 073059
[27] Uhrig G S 2007 *Phys. Rev. Lett.* **98** 100504
[28] Qian X, Sun Z and Zhou N 2022 *Phys. Rev. A* **105** 012431
[29] Li H B, Zheng Q, Zhi Q J and Li Y 2022 *Phys. Rev. A* **105** 042612
[30] Uhrig G S 2008 *New J. Phys.* **10** 083024
[31] Leggett A J, Chakravarty S, Dorsey A T, Fisher M P A, Garg A and Zwerger W 1987 *Rev. Mod. Phys.* **59** 1
[32] Lin Y C, Yang P Y and Zhang W M 2016 *Sci. Rep.* **6** 34804
[33] Nalbach P, Braun D and Thorwart M 2011 *Phys. Rev. E* **84** 041926
[34] Ringsmuth A K, Milburn G J and Stace T M 2012 *Nat. Phys.* **8** 562
[35] De Silva N, Warnakula T, Gunapala S D, Stockman M I and Premaratne M 2021 *J. Phys.: Condens. Matter* **33** 145304
[36] Correa L A, Perarnau-Llobet M, Hovhannisyan K V, Hernández-Santana S, Mehboudi M and Sanpera A 2017 *Phys. Rev. A* **96** 062103
[37] He D, Thingna J and Cao J 2018 *Phys. Rev. B* **97** 195437
[38] Palma G M, antti Suominen K and Ekert A 1996 *Proc. R. Soc. Lond. A.* **452** 567
[39] Austin S, Zahid S and Chaudhry A Z 2020 *Phys. Rev. A* **101** 022114
[40] Niu C and Yu S 2023 *Chin. Phys. Lett.* **40** 110301
[41] Braunstein S L and Caves C M 1994 *Phys. Rev. Lett.* **72** 3439
[42] Luo M, Liu W, Chen Y, Han S and Gao S 2022 *Chin. Phys. B* **31** 050304
[43] Kenfack L T, Gueagni W D W, Tchoffo M and Fai L C 2021 *Eur. Phys. J. Plus* **136** 1